International Journal of Mechatronics and Applied Mechanics
2025, Issue 20, Vol. 1

STIFFNESS MODELING OF INDUSTRIAL ROBOTS BASED ON MACHINE LEARNING ALGORITHMS

*Pengzhan Zhao[1] and Fangli Qing[1]**
[1]School of Information and Inte1ligent Manufacturing, Chongqing City Vocational College, Chongqing, 402160, China

Abstract: The low stiffness of industrial robots leads to poor machining accuracy and quality. However, existing industrial robot stiffness models lack efficiency and generalization, making it difficult to ensure prediction accuracy. Therefore, this study introduces an industrial robot stiffness model based on the Grey Wolf Optimizer and Multi-layer Perceptron. The proposed model fully utilizes the global optimization capability of the Grey Wolf Optimizer and the computational power of the Multi-layer Perceptron. This enables precise and efficient stiffness prediction for industrial robots. The experimental findings demonstrate that the model put forward reaches a prediction accuracy of 93.5% with a loss rate of only 0.91%, significantly outperforming the comparison models. In real-world industrial robot stiffness prediction, the model achieves an accuracy of 93.2%, and in calculating the deformation values at the robot's end position, the error rate reaches as low as 2.89%, demonstrating a significant advantage over the comparison models. These findings suggest that the proposed model demonstrates outstanding predictive accuracy and stability in the context of industrial robot stiffness modeling. effectively addressing the issues of accuracy and generalization in existing modeling methods. This study provides new insights and approaches for stiffness modeling in industrial robots in the manufacturing industry, contributing to the advancement of intelligent and efficient manufacturing processes.

Keywords: Industrial robots; Grey wolf optimizer; Multi-layer perceptron; Stiffness modeling; End deformation; Machine learning; Neural networks.

1. Introduction

As the manufacturing industry evolves rapidly, there has been an increasing demand for higher efficiency, precision, and cost-effectiveness in production methods. As an advanced machining tool, industrial robots offer advantages such as a large working space, high production efficiency, and low manufacturing costs [1]. Nevertheless, the low stiffness of industrial robots leads to reduced machining accuracy and compromised quality. Additionally, their stiffness is influenced by multiple external factors, including environmental conditions and friction, making precise acquisition challenging [2]. Existing industrial robot stiffness models have attempted to compensate for machining accuracy by incorporating various influencing factors. However, the excessive introduction of parameters compromises model efficiency and generalization [3]. Therefore, an accurate and efficient method for predicting robot stiffness is urgently needed.

As artificial intelligence continues to advance rapidly, machine learning-based models have shown distinct advantages. Among them, the Multi-layer Perceptron (MLP) exhibits strong generalization capabilities due to its self-learning and self-adaptive abilities. Meanwhile, the Grey Wolf Optimizer (GWO) is known for its superior optimization capability, which can enhance the operational speed and accuracy of MLP by optimizing its parameters [4-5]. The integration of these two methods in stiffness modeling enables the rapid generation of initial solutions, further improving prediction efficiency and accuracy. Based on this, this study introduces an industrial robot stiffness model based on the GWO-MLP.

The model aims to achieve accurate stiffness prediction under complex production environment conditions. By improving the efficiency and generalization of existing stiffness models, this study offers both theoretical support and technical validation for the advancement of industrial robot stiffness prediction, further promoting the intelligent advancement of the manufacturing industry.

https://doi.org/10.17683/ijomam/issue20.28

2. Related Works

As a nonlinear mapping model, MLP has advantages such as strong learning ability and good generalization performance, making it applicable to various fields. Scholars worldwide have conducted extensive research on MLP and have made significant progress. For instance, Zheng H et al. addressed the issue of high training time and computational cost in convolutional neural networks for computer vision tasks such as fruit recognition. They proposed a method for identifying the appearance quality of strawberries based on the Swin Transformer and MLP. Experimental results showed that this method achieved an accuracy of 98.45% with a training time of only 16.79 seconds, demonstrating excellent performance in strawberry appearance quality classification [6]. Al Bataineh A's team tackled the problem that MLP often fails to obtain an optimal solution by proposing a clonal selection algorithm capable of efficiently exploring complex large spaces to approach the global optimum. Research findings indicated that, compared to other training methods, using the clonal selection algorithm improved the performance of MLP [7]. Altay O et al. addressed challenges in gradient-based backpropagation methods, such as getting stuck in local minima, rapid convergence, and low sensitivity to initialization. They proposed an enhanced GWO integrated with MLP. Experimental results showed that this approach outperformed comparison algorithms, including Particle Swarm Optimization, Whale Optimization Algorithm, and Ant Lion Optimization [8]. As a bio-inspired algorithm, GWO has attracted significant research attention due to its excellent convergence speed and search capability. For example, Meidani K et al. addressed the low computational efficiency of population-based metaheuristic optimization algorithms by introducing an improved adaptive GWO. This version adjusts the exploration and exploitation parameters dynamically throughout the optimization process, relying on the fitness history of the candidate solutions. Experimental results demonstrated that the adaptive GWO proved to be an effective optimization algorithm [9]. Zamfirache I A's team tackled the issue of high error rates in traditional machine learning methods by proposing a novel reinforcement learning-based control method. This approach employed policy iteration and a metaheuristic GWO to train neural networks. Experimental results indicated that GWO effectively eliminated steady-state control errors, ensuring the convergence of the objective function [10].

Moreover, with the rapid development of the manufacturing industry, the construction of stiffness models for industrial robots has emerged as a prominent topic in the field. Scholars worldwide have conducted extensive research and proposed various solutions. For instance, Cui G et al. addressed the issue of low structural stiffness in industrial robots during operation, which leads to poor surface quality and low precision of machined parts. They put forward a dynamic modeling and vibration prediction approach for industrial robots subjected to machining forces. The results confirmed that the proposed method was effective in predicting machining vibrations of industrial robots [11]. Li Z's team addressed the issue of unstable positioning accuracy in flexible tracked drilling robots, a challenge that hinders their broader adoption in high-precision machining sectors like aircraft assembly. They introduced an equivalent stiffness model to predict the incremental error across the entire process station. Experimental results demonstrated that the incremental error compensation method led to a 68.67% reduction in the total error [12]. Kim D C et al. tackled the challenge of achieving high dimensional accuracy and improving the dynamic performance of industrial robots. They introduced an MLP model for predicting the primary natural frequency and dynamic stiffness of industrial robot tool tips. Experimental results showed that the model significantly improved the machinability of CFRP robots [13]. Kozakiewicz B's team studied the negative stiffness exhibited by modern robotic springs, which makes prediction and control difficult. They proposed a variable stiffness brake. Experimental results suggested that the entire variable stiffness brake is promising and has potential for further development. Its miniaturized design makes it suitable for applications in modern robotic mechanisms [14]. Lu Y et al. addressed the difficulty in improving the accuracy of inverse dynamic models for robots. They proposed an external force estimation method that employs a semi-parametric friction model and configuration optimization using Jacobian condition numbers to reduce modeling errors and their negative impacts. Experimental results demonstrated that this method enhanced online force estimation performance by 48.28% [15].

In summary, optimizing the parameters of MLP can improve the prediction efficiency and accuracy of the model, providing a new approach to address the computational challenges caused by numerous complex parameters. Although existing research has achieved certain progress in the field of industrial robot stiffness modeling, most studies focus on model structure design or specific application cases, lacking systematic exploration of parameter optimization for MLP. Moreover, the selection of optimization algorithms remains limited, and a stable and effective general optimization strategy has yet to be established. In addition, some existing methods still suffer from unstable prediction accuracy and slow convergence when dealing with high-dimensional input features or complex nonlinear relationships. To enhance the generalization ability and convergence stability of the model in complex industrial scenarios, this study proposes a GWO-MLP-based stiffness modeling method by integrating Grey Wolf Optimizer with MLP. The aim is to achieve an efficient, accurate, and generalizable stiffness prediction model for industrial robots, addressing the dual demands of precision and real-time performance in intelligent manufacturing.

3. Construction of MLP-based industrial robot stiffness model combined with GWO

3.1 Improved MLP Design with GWO Integration

MLP, as a machine learning algorithm, has strong learning and adaptive capabilities, making it uniquely advantageous. The structure of MLP is simple, yet it has strong computational power, enabling it to effectively solve nonlinear problems, handle classification tasks, and perform regression analysis [16]. MLP demonstrates excellent and profound application value in various fields such as image vision, factory production, and semantic understanding [17]. Its network structure is expressed by Figure 1.

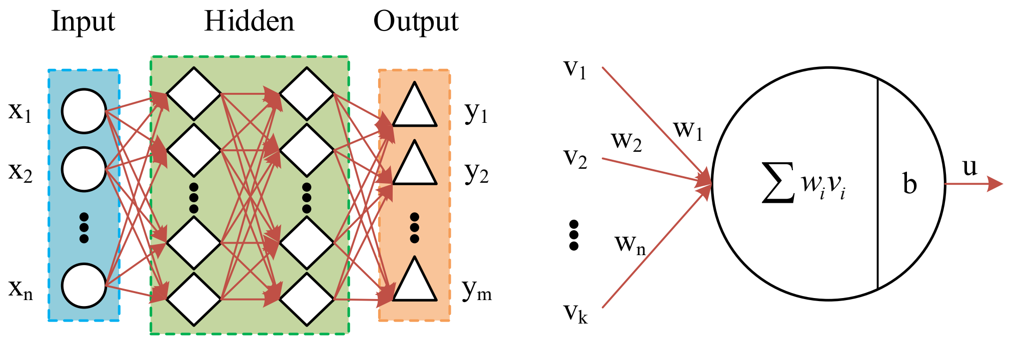

(a) MLP network structure diagram (b) Neuron model

Figure 1: MLP network structure diagram and neuron model

As shown in Figure 1(a), MLP consists of an input layer, several hidden layers, and an output layer. Initially, the input layer transmits the vector into the hidden layers, where it is processed and then output after being processed by the neurons in the hidden layers. The model of the neuron is depicted in Figure 1(b). In the MLP architecture, the input layer nodes are responsible for data input, while the remaining nodes are neurons with built-in activation functions. Each neuron is equipped with its own weight parameters and bias terms. This model strictly follows the feedforward neural network mechanism. Through this ordered data transmission process, it enables step-by-step fine-grained processing and deep feature extraction of the input data, thereby completing complex pattern recognition and data analysis tasks. The final output result of the model is shown in Equation (1).

$$Y_n^k = f_n^k(W_{ni}^k * Y^{k-1} + b_n^k) \tag{1}$$

In Equation (1), Y represents the neuron output, W denotes the connection weights, b represents the neuron bias term, k refers to the k-th layer of MLP, n indicates the n-th neuron in the corresponding layer, and f represents the activation function. The activation function used in this model is the widely applied ReLU, which enables fast gradient computation, as shown in Equation (2).

$$\mathrm{Re}LU(X) = \max(0, x) \tag{2}$$

In Equation (2), x represents the input value, while $\mathrm{Re}LU(X)$ denotes the output after applying the linear rectified function. From the above formulas, it can be seen that the weight parameters W and bias terms b have a decisive influence on the final output. To accurately find the optimal values of these parameters, they are computed and solved through an appropriate optimization algorithm. GWO, as a bio-inspired algorithm, demonstrates excellent performance in search capability.

The process of obtaining the optimal solution is shown in Figure 2 [18].

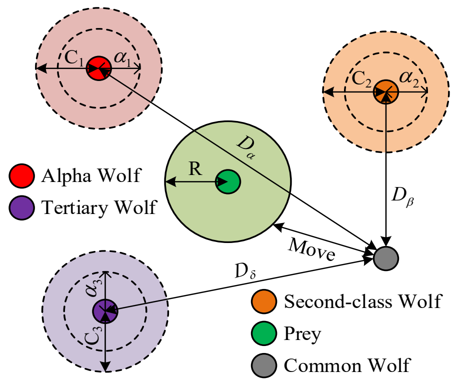

Figure 2: Diagrammatic sketch of the process of GWO obtaining the optimal solution

As shown in Figure 2, GWO is inspired by the social hierarchy within a gray wolf pack, where each wolf's influence during hunting is determined by its rank. The alpha wolf holds the highest level of influence, followed by the beta and delta wolves, with the omega wolf having the least influence. The hunting action of the wolf pack consists of three steps. The first is the scouting and tracking phase, during which the gray wolf pack carefully observes, tracks, and locks in the prey's position while gradually closing in on it.

The update of the gray wolf's position during this process is shown in Equation (3).

$$\begin{cases} D = \left| CX_p(l) - X(l) \right| \\ X(l+1) = X_p(l) - AD \end{cases} \tag{3}$$

In Equation (3), D represents the position of the wolf pack, $X_p(l)$ denotes the hunting vector, l represents the number of iterations, and $X(l)$ and $X(l+1)$ represent the position vectors after the iterations. The next phase is the encirclement stage, where the alpha wolf plays a leading role, directing the pack to drive the prey from multiple directions, gradually reducing the prey's escape space, making it difficult for the prey to break free. Finally, the attack phase begins, in which the confrontation between the gray wolves and the prey essentially becomes a continuous process of exploration and seeking the optimal solution to successfully capture the prey. To enhance the efficiency and accuracy of MLP computations, the study proposes the introduction of an improved MLP with GWO, and the operational process of GWO-MLP is shown in Figure 3.

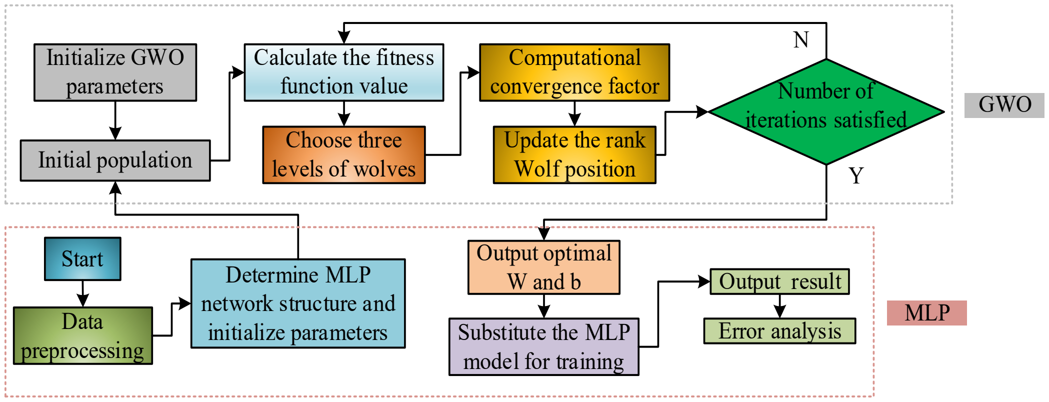

Figure 3: Schematic diagram of the operation process of GWO-MLP

As shown in Figure 3, in the initial data processing phase, GWO-MLP employs a dimensionality reduction factor analysis method to select the primary data with higher weight values, successfully reducing the redundant input variables and thus improving model training efficiency and reducing data redundancy. During the model construction and parameter initialization phase, the number of hidden layers in the MLP is established first, followed by the sequential determination of the number of neurons in eac layer. The parameters are then initialized. Based on GWO, wolves are selected sequentially as the alpha, second-level, and third-level wolves according to their fitness values within the population.

After that, the convergence factor is calculated. In the entire population, the position update formula for gray wolves is expressed by Equation (4).

$$\begin{cases} X_{i,\alpha}(t+1) = X_\alpha(t) - AD_\alpha \\ X_{i,\beta}(t+1) = X_\beta(t) - AD_\beta \\ X_{i,\delta}(t+1) = X_\delta(t) - AD_\delta \end{cases} \tag{4}$$

In Equation (4), $X_i(t+1)$ represents the updated position of the gray wolf, A represents the perturbation factor, D represents the individual distance between gray wolves, and $X(t)$ represents the position of the prey. After determining the position of the gray wolves based on the position update formula, the entire population's position is adaptively updated.

When the number of iterations reaches the predefined maximum limit, the optimal values for W and b are acquired. Finally, the optimal parameters are input into the MLP for training, and error analysis is conducted on the training results to evaluate the model's performance and accuracy. The error analysis uses Root Mean Square Error (RMSE) and Mean Absolute Error (MAE) for calculation and judgment, and their mathematical expressions are shown in Equation (5).

$$\begin{cases} RMSE = \sqrt{(1/n)\sum_{i=1}^{n}(\hat{y}_i - y_i)^2} \\ MAE = (1/n)\sum_{i=1}^{n}\left|\hat{y}_i - y_i\right| \end{cases} \tag{5}$$

In Equation (5), $\hat{y}_i$ represents the predicted value, n represents the total number of samples, and y_i represents the actual value.

3.2 Construction of Industrial Robot Stiffness Model based on GWO-MLP

Once constructed, the GWO-MLP model is further applied to the development of the industrial robot stiffness model. The construction of the robot stiffness model needs to incorporate the force Jacobian matrix. During robot operation in production, the end-effector of the robot interacts with external factors, generating related forces [19]. The movements of the robot's joints apply torques and forces, which are transmitted through the connections to the end-effector, counteracting the external forces and torques it faces. By applying the principle of virtual work, it can be assumed that when the robot is subjected to external forces, its joints experience virtual displacements. The virtual displacement of the end-effector is shown in Figure 4 [20].

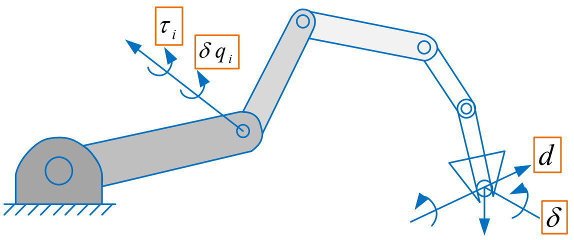

Figure 4: Schematic diagram of virtual displacement of the end effector

As shown in Figure 4, after the virtual displacement occurs, let the industrial robot joints be subjected to a force of magnitude τ_i, and the end-effector be subjected to a force of magnitude F. The virtual work is mathematically formulated in Equation (6).

$$\delta W = \tau^T \delta q - F^T \delta X \tag{6}$$

In Equation (6), δW represents the virtual work done by the robot, and τ represents the joint torque. According to the principle of displacement, when the object is in a balanced state, the virtual work done is zero. Therefore, the above equation can be transformed into Equation (7).

$$\delta W = (\tau - J^T F)^T \delta q \tag{7}$$

In Equation (7), δq represents the displacement variables of the industrial robot joints. When $\delta W = 0$ occurs, the joint torque is shown in Equation (8).

$$\tau = J^T F \tag{8}$$

In Equation (8), J^T represents the force Jacobian matrix. From this, it can be concluded that there is a mapping relationship between the force and velocity Jacobian matrices of the robot in the static condition. Based on the force Jacobian matrix of the industrial robot, the modeling is carried out using the Modified_DH method, which can effectively reduce the occurrence of coordinate system overlap. A schematic diagram of this method is shown in Figure 5.

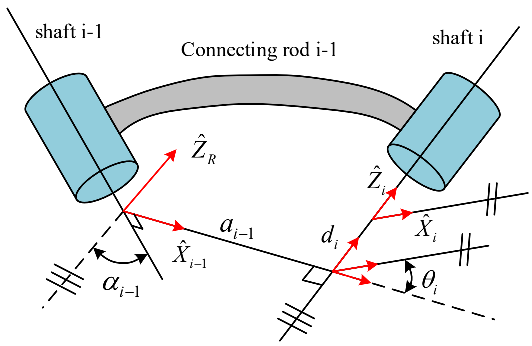

Figure 5: Schematic diagram of Modified_DH method

As shown in Figure 5, when the serial industrial robot has random degrees of freedom and the constant parameters α_i, a_i, and d_i are determined, the transformation matrix from the end-effector to the reference coordinate can be obtained based on θ_i. The homogeneous transformation matrix is shown in Equation (9).

$$T_N^0 = T_1^0 T_2^1 \ldots T_N^{N-1} \tag{9}$$

In Equation (9), T represents the homogeneous transformation matrix of adjacent joints of the industrial robot. When the robot end-effector is equipped with production tools, such as engraving tools, various behavioral change values of the end-effector coordinates M are obtained through calculation, and the reference direction is reasonably set. Based on this, the transformation matrix from the N -th joint to this position can be derived according to relevant theories. Therefore, the transformation matrix of the end-effector tool is shown in Equation (10).

$$T_M^0 = T_N^0 T_M^N \tag{10}$$

In Equation (10), T_M^N represents the transformation matrix from the N -th joint to the end-effector coordinates M . Based on this, the constructed GWO-MLP is introduced to fit the stiffness of the industrial robot, thereby building the industrial robot stiffness model. The operational flow of the GWO-MLP-based industrial robot stiffness model is shown in Figure 6.

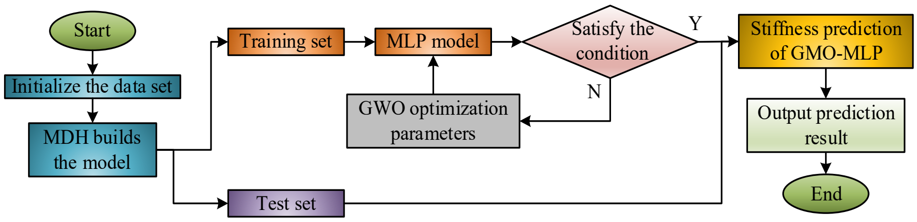

Figure 6: GWO-MLP-based stiffness model operation flow chart

As shown in Figure 6, the workflow of this model begins with data processing, where the robot's model parameters, position, coordinate system, and force Jacobian matrix are input into the model. The model construction then proceeds using the Modified_DH method. During the construction process, the Cartesian and operational stiffness of the industrial robot are set based on the differences in the reference frames defined for the robot. The mathematical expression of the traditional mapping relationship between the two is shown in Equation (11).

$$K_X = J^{-T} K_\theta J^{-1} \tag{11}$$

In Equation (11), K_X represents the Cartesian stiffness of the robot, J represents the Jacobian matrix, and K_θ represents the operational stiffness. In actual production processes, the Cartesian stiffness of industrial robots is easily interfered with by external load environments. Therefore, after defining the operational stiffness, stiffness compensation needs to be performed. The mathematical expression for this compensation is shown in Equation (12).

$$K_C = \left[\frac{\partial J^T}{\partial \theta_1} w \ \frac{\partial J^T}{\partial \theta_2} w \ldots \ \frac{\partial J^T}{\partial \theta_6} w \right] \tag{12}$$

In Equation (12), K_C represents the stiffness compensation matrix, θ represents the robot's torsional deformation, and w represents the torque vector. Therefore, the mathematical expression for the mapping relationship after stiffness compensation is shown in Equation (13).

$$K_X = J^{-T} (K_\theta - K_C) J^{-1} \tag{13}$$

In Equation (13), K_X represents the Cartesian stiffness after stiffness compensation.

The stiffness data is then divided into training and testing sets, with the training set being input into the MLP for iterative training. After each iteration, the convergence state of the algorithm is analyzed. If the convergence condition is met, the process proceeds to the next step in an orderly manner. If not, the iteration continues. When the population's fitness value is at a low level, the search range of GWO gradually shrinks. Once the required condition is met, stiffness prediction is output. If the condition is not met, parameter optimization is performed via GWO, and the calculation is repeated until the condition is satisfied.

4. Verification of GWO-MLP and its Industrial Robot Stiffness Model

4.1 Performance Verification of Improved MLP with GWO Integration

To validate the efficiency and accuracy of the proposed GWO-MLP, as well as its ability to meet the requirements of the industrial robot stiffness model, the study compared it with commonly used machine learning algorithms, including Radial Basis Function (RBF) neural network, Support Vector Machine (SVM), and Random Forest (RF) algorithms. The machine learning algorithms were trained and tested on a Windows 10 system equipped with an Intel(R) Core(TM) i5-7300HQ processor. The experimental parameters are outlined in Table 1.

Building on the experimental environment and model parameters outlined above, the study assessed the performance of the models by comparing key metrics such as prediction accuracy, loss rate, coefficient of determination (R^2), RMSE, and MAE across the four algorithms. Initially, the accuracy and loss rate of the four algorithms were compared, with the experimental results presented in Figure 7.

Table 1 Experimental parameter configuration for each module in the model

Trait	Parameter
Enter the number of parameter features	18
Output the number of parameter features	6
Three-layer network	25-45-22
Activation function	ReLu-ReLu-Tanh
Optimizer	RMSprop optimization algorithm
Loss function	MSE function
Learning rate	0.1
Momentum	0.9

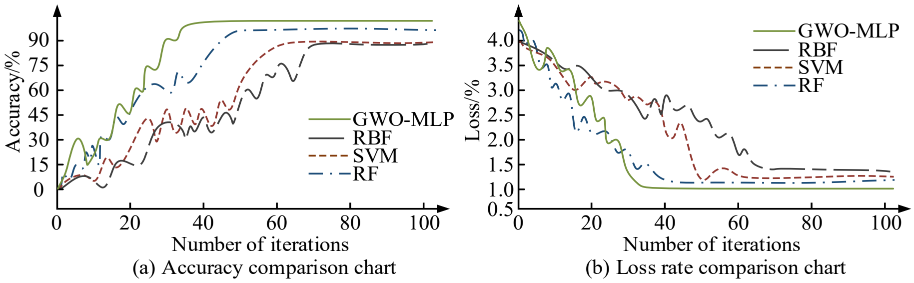

Figure 7: Experimental results of accuracy and loss rate

As shown in Figure 7(a), after 30 iterations on the training dataset, the accuracy of GWO-MLP stabilized at 93.5%. The other three algorithms showed greater fluctuation until around 50 iterations, after which their accuracy began to stabilize. By the 70th iteration, the accuracy of the four algorithms ranked from highest to lowest as follows: GWO-MLP with 93.5%, RBF with 90.2%, SVM with 86.5%, and RF with 85.3%. GWO-MLP achieved the highest accuracy. Figure 7(b) shows that after 30 iterations on the training dataset, the loss rate of GWO-MLP and RF stabilized at 0.91% and 1.02%, respectively. At this point, GWO-MLP had a lower loss rate than RF. RBF and SVM gradually stabilized their loss rates after 60 iterations. After 60 iterations, the loss rates of the four algorithms ranked from lowest to highest as follows: GWO-MLP with 0.91%, RF with 1.02%, RBF with 1.23%, and SVM with 1.43%. GWO-MLP consistently had the lowest loss rate. This data indicates that the proposed algorithm outperformed the others, achieving the highest computational accuracy. To provide a more comprehensive evaluation of each algorithm's predictive performance, the study also compared the algorithms using R^2, RMSE, and MAE, as shown in Figure 8.

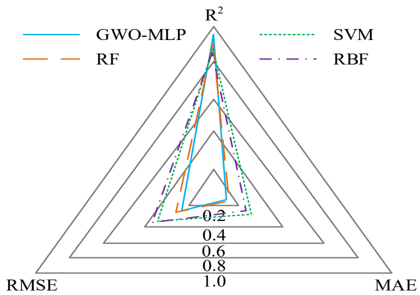

Figure 8: Comparison of prediction effect of four algorithms

As shown in Figure 8, the research results for industrial robot stiffness prediction indicated that GWO-MLP significantly outperformed the comparison algorithms across all three evaluation metrics. Specifically, GWO-MLP achieved an R^2 of 0.9632, which was approximately 3% higher than RF's 0.9234, RBF's 0.9024, and SVM's 0.9123. Additionally, GWO-MLP had the lowest RMSE and MAE, reaching values of 0.2166 and 0.1365, respectively, demonstrating its superior data fitting ability. These results strongly confirmed that GWO-MLP offers higher prediction accuracy than the other three methods for industrial robot stiffness prediction, and also effectively validated the use of GWO to optimize MLP parameters.

4.2 Performance Verification of Industrial Robot Stiffness Model based on GWO-MLP

After verifying the predictive performance of GWO-MLP, the study further compared the developed model with RBF, SVM, and RF algorithms to assess the practical application value of the GWO-MLP-based industrial robot stiffness model. The study predicted industrial robot joint torsion deformation using the four models on the training dataset, and the comparison of the prediction results is shown in Figure 9.

As shown in Figure 9(a), the analysis of the GWO-MLP stiffness model's fitting performance on the training dataset revealed that the model exhibited excellent fitting performance. Overall, the model achieved high precision in fitting, with only a few points of large deformation showing small errors. The overall prediction accuracy reached 93.2%.

Observing Figure 9(b), RF showed lower prediction values at some points with large deformation, though it still achieved a prediction accuracy of 85%. In Figure 9(c), the RBF model showed lower prediction accuracy and struggled to accurately predict the actual values of the training dataset, also facing the issue of predicting the deformation direction incorrectly. Even under large deformation conditions, the model was unable to accurately predict the deformation. In summary, the GWO-MLP stiffness model proposed in the study demonstrated the best fitting performance, closely matching the deformation of the industrial robot. To further verify the effectiveness of the proposed stiffness prediction model, the study used the four models to calculate the end effector deformation values of the industrial robot, setting six different robot poses. The calculated values were compared with the measured values and error rates, with the comparison results shown in Figure 10.

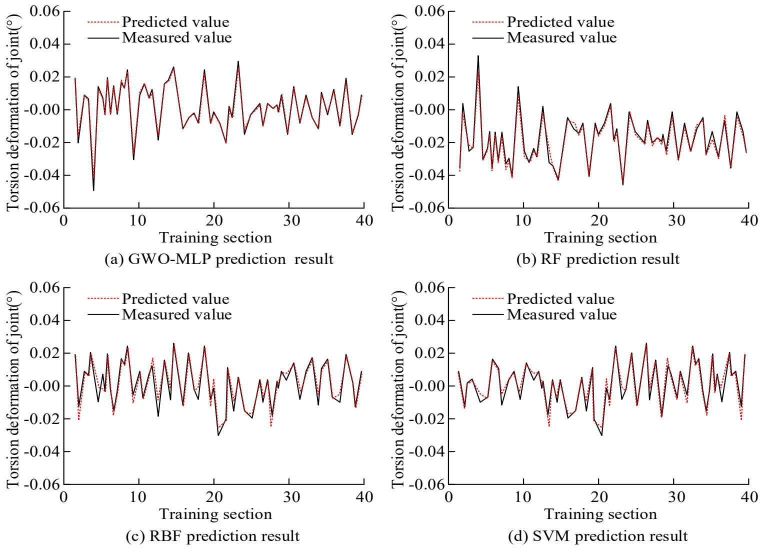

Figure 9: Comparison of prediction results of joint torsion deformation

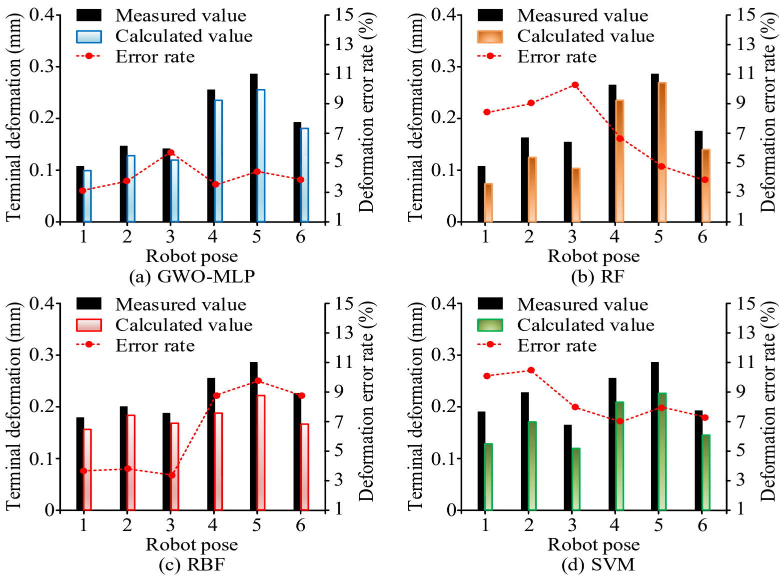

Figure 10: Comparison results of calculated values, measured values and error rates

As shown in Figure 10(a), the calculated values of the GWO-MLP stiffness model exhibited a small error compared to the actual values. The error was relatively stable and fluctuated within a certain range, with the minimum error reaching 2.89%. In Figure 10(b), the RF stiffness model showed larger errors when the actual values were small, while the error rate decreased when the actual values were larger, with the lowest error rate reaching 3.93%. In Figure 10(c), the RBF stiffness model displayed the opposite trend compared to the RF model, with the highest error rate reaching 10.23% when the actual values were larger.

As shown in Figure 10(d), the SVM model's error rate was worse than that of the other models. In summary, the GWO-MLP stiffness model proposed in the study demonstrated significantly better performance in predicting the end effector deformation of industrial robots compared to the other algorithms, confirming its feasibility for predicting the stiffness of industrial robots. To further validate the applicability of the proposed model for stiffness prediction, the study applied it to predict the linear joint stiffness of industrial robots, comparing the predicted translation and torsion errors with the other three models. The results are shown in Figure 11.

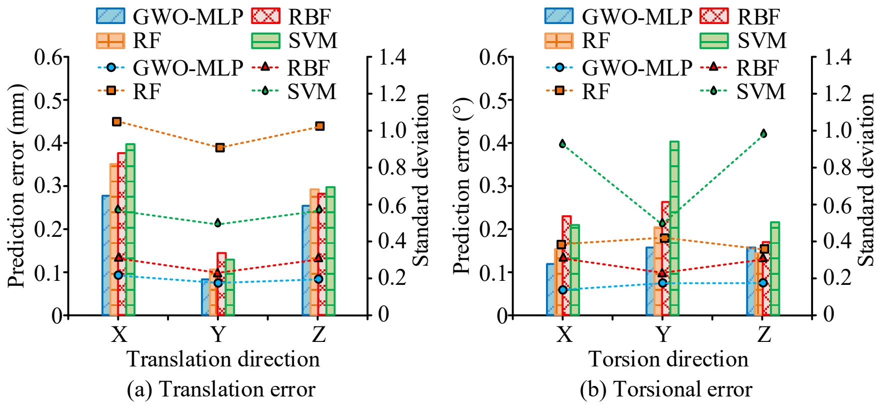

Figure 11: Experimental results of translation error and torsion error

As shown in Figure 11(a), for the translation errors of the robot's linear joints, the GWO-MLP stiffness model proposed by the study exhibited the smallest errors in all three directions. The translation errors in the X, Y, and Z axes were 0.28mm, 0.08mm, and 0.26mm, respectively, all significantly lower than those of the comparison algorithms. Furthermore, the standard deviations of the GWO-MLP model were lower than those of the comparison algorithms, suggesting that its predictions exhibited less variability and reflected the most consistent performance. In Figure 11(b), for the robot's linear joint torsion errors, the GWO-MLP stiffness model also showed the smallest errors, with torsion errors of 0.12°, 0.17°, and 0.18° in the three directions, all notably better than those of the comparison algorithms, while the SVM model performed the worst. In conclusion, the GWO-MLP stiffness model proposed by the study demonstrated outstanding performance in predicting various errors for industrial robot joints, with both higher accuracy and stability compared to the other algorithms.

5. Conclusions

To address the issues of prediction efficiency and accuracy in existing industrial robot stiffness models, this study innovatively proposed a GWO-MLP-based industrial robot stiffness model. By leveraging the global search ability of GWO to optimize the key parameters of MLP, the model achieved precise and efficient predictions for industrial robot stiffness. The experimental results indicated that the proposed GWO-MLP stiffness model outperformed the comparison methods across various evaluation metrics, such as prediction accuracy, loss rate, R^2, RMSE, and MAE. Specifically, the prediction accuracy reached 93.5%, and the loss rate was 0.91%, demonstrating its excellent computational performance. The R^2, RMSE, and MAE values were 0.9632, 0.2166, and 0.1365, respectively, indicating the high precision of the predictions. In practical applications, the proposed GWO-MLP stiffness model achieved a prediction accuracy of 93.2% in robot joint torsion deformation prediction, with the lowest error rate of 2.89% in calculating robot end position deformation values, and the smallest prediction errors in linear joint translation and torsion error experiments. Overall, the GWO-MLP-based industrial robot stiffness model demonstrated excellent stiffness prediction capability, stability, and generalization, meeting the manufacturing industry's need for industrial robot stiffness detection. Although the model performed excellently in terms of performance and application, it was developed using only one model of industrial robot, and its universal applicability requires further investigation. Future work will involve conducting experiments with different models of industrial robots to further improve and upgrade the model, continuously enhancing its prediction universality and effectiveness.

Finally, to further verify the effectiveness of GWO in optimizing MLP parameters, this study selected three mainstream intelligent optimization algorithms—Particle Swarm Optimization (PSO), Genetic Algorithm (GA), and Whale Optimization Algorithm (WOA)—and constructed corresponding optimizer-MLP hybrid models for comparison with GWO.

The modeling performance of these combinations was evaluated in the task of industrial robot stiffness prediction. All optimizers were implemented under the same MLP network structure and parameter settings to ensure fairness.

The experiments were conducted using an industrial robot dataset with 18 input features and 6 output features. The MLP adopted a three-layer architecture (25-45-22), with ReLU-ReLU-Tanh as the activation functions and MSE as the loss function.

The number of optimization iterations was set to 100, and each experiment was repeated 10 times with average values used to improve stability. The experimental results are shown in Table 2.

Table 2 Comparison of stiffness prediction performance using MLP optimized by different algorithms

Model Combination	Accuracy (%)	Coefficient of Determination (R^2)	Root Mean Square Error (RMSE)	Mean Absolute Error (MAE)	Convergence Iterations
GWO-MLP	93.5	0.9632	0.2166	0.1365	36
PSO-MLP	91.3	0.9415	0.2731	0.1742	45
GA-MLP	89.7	0.9244	0.2946	0.1885	53
WOA-MLP	90.2	0.9336	0.2827	0.1813	49

As observed from Table 2, the GWO-MLP model outperformed the other three optimization algorithms across multiple key performance metrics, including accuracy, R^2, RMSE, and MAE. Specifically, GWO-MLP achieved a prediction accuracy of 93.5%, an R^2 value of 0.9632, an RMSE of 0.2166, and an MAE of 0.1365, demonstrating the best fitting precision and error control capability. Moreover, GWO reached convergence within only 36 iterations, significantly faster than PSO (45 iterations), GA (53 iterations), and WOA (49 iterations), indicating superior convergence efficiency and stability. These findings further validate the global search advantages of GWO in complex nonlinear modeling scenarios, highlighting its suitability for high-precision stiffness prediction tasks in industrial robotics.

Fundings

The research is supported by: Project of science and technology research program of Chongqing Education Commission of China. (No KJQN202303910); (No KJQN202303910).

References

[1] Xu L, Mao W, Zhu L, Xu J, Sun Y. Tool orientation and redundancy integrated planning method constrained by stiffness for robotic machining of freeform surfaces. The International Journal of Advanced Manufacturing Technology, 2022, 121(11): 8313-8327.

[2] Tepper C, Matei A, Zarges J, Ulbrich S, Weigold M. Optimal design for compliance modeling of industrial robots with bayesian inference of stiffnesses. Production Engineering, 2023, 17(5): 643-651.

[3] Song W, Yang X, Liu H, Gao X, Lei Y, Cao J. A new method for calculating time-varying torsional stiffness of RV reducers with variable loads and tooth modifications. Journal of Field Robotics, 2023, 40(6): 1339-1345.

[4] Yaylacı M, Yaylacı E U, Özdemir M E, Öztürk Ş, Sesli H. Vibration and buckling analyses of FGM beam with edge crack: Finite element and multilayer perceptron methods. Steel and Composite Structures, An International Journal, 2023, 46(4): 565-575.

[5] Makhadmeh S N, Alomari O A, Mirjalili S, Al-Betar M A, Elnagar A. Recent advances in multi-objective grey wolf optimizer, its versions and applications. Neural Computing and Applications, 2022, 34(22): 19723-19749.

[6] Zheng H, Wang G, Li X. Swin-MLP: A strawberry appearance quality identification method by Swin Transformer and multi-layer perceptron. Journal of Food Measurement and Characterization, 2022, 16(4): 2789-2800.

[7] Al Bataineh A, Kaur D, Jalali S M J. Multi-layer perceptron training optimization using nature inspired computing. IEEE Access, 2022, 10(6): 36963-36977.

[8] Altay O, Varol Altay E. A novel hybrid multilayer perceptron neural network with improved grey wolf optimizer. Neural Computing and Applications, 2023, 35(1): 529-556.

[9] Meidani K, Hemmasian A P, Mirjalili S, Barati Farimani A. Adaptive grey wolf optimizer. Neural Computing and Applications, 2022, 34(10): 7711-7731.

[10] Zamfirache I A, Precup R E, Roman R C, Petriu E M. Policy iteration reinforcement learning-based control using a grey wolf optimizer algorithm. Information Sciences, 2022, 585(3): 162-175.

[11] Cui G, Li B, Tian W, Liao W, Zhao W. Dynamic modeling and vibration prediction of an industrial robot in manufacturing. Applied Mathematical Modelling, 2022, 105(8): 114-136.

[12] Li Z, Tian W, Hu J, et al. Deformation error compensation by stiffness model of mechanical joint on a flexible track drilling robot for aircraft assembly. The International Journal of Advanced Manufacturing Technology, 2023, 127(11-12): 5863-5878.

[13] Kim D C, Seo J, Park H W. Dynamic performance of industrial robots in the secondary carbon fiber-reinforced plastics machining. Journal of Manufacturing Processes, 2023, 103(2): 120-135.

[14] Kozakiewicz B, Winiarski T. Spring based on flat permanent magnets: design, analysis and use in variable stiffness actuator. Facta Universitatis, Series: Mechanical Engineering, 2023, 21(1): 101-120.

[15] Lu Y, Shen Y, Zhuang C. External force estimation for industrial robots using configuration optimization. Automatika: časopis za automatiku, mjerenje, elektroniku, računarstvo i komunikacije, 2023, 64(2): 365-388.

[16] Xie X, Pu Y F, Wang J. A fractional gradient descent algorithm robust to the initial weights of multilayer perceptron. Neural Networks, 2023, 158(4): 154-170.

[17] Ghimire S, Nguyen-Huy T, Prasad R, Deo R C, Casillas-Pérez D, Salcedo-Sanz S, Bhandari B. Hybrid convolutional neural network-multilayer perceptron model for solar radiation prediction. Cognitive Computation, 2023, 15(2): 645-671.

[18] Sharma I, Kumar V, Sharma S. A comprehensive survey on grey wolf optimization. Recent Advances in Computer Science and Communications (Formerly: Recent Patents on Computer Science), 2022, 15(3): 323-333.

[19] Zeng X, Zhu G, Gao Z, Ji R, Ansari J, Lu C. Surface polishing by industrial robots: a review. The International Journal of Advanced Manufacturing Technology, 2023, 125(9): 3981-4012.

[20] Zhang J, Cong M, Liu D, Du Y, Ma H. A lightweight variable stiffness knee exoskeleton driven by shape memory alloy. Industrial Robot: the international journal of robotics research and application, 2022, 49(5): 994-1007.